Acta Biochimica Polonica

Vol. 44 No. 4/1997

673–678

QUARTERLY

This paper is dedicated to Professor Włodzimierz Ostrowski

Prostatic acid phosphatase: structural aspects of inhibition by L-(+)-tartrate ions*

Leslie Lovelace[1], Krzysztof Lewiński[2], Clarissa G. Jakob[3], Radosława Kuciel[4], Włodzimierz Ostrowski[4] and Łukasz Lebioda[1]✉

[1]*Department of Chemistry and Biochemistry, University of South Carolina, Columbia, SC 29208, U.S.A.*
[2]*Faculty of Chemistry, Jagiellonian University, R. Ingardena 3, 30-060 Cracow, Poland*
[3]*Department of Chemistry, Davidson College, Davidson NC, U.S.A.*
[4]*Institute of Medical Biochemistry, Collegium Medicum, Jagiellonian University, M. Kopernika 7, 31-034 Cracow, Poland*

Key words: prostatic acid phosphatase, crystal structure, tartrate, electrostatic potentials

The crystal structure of the complex between rat-prostatic acid phosphatase (PAP) and L-(+)-tartrate (Lindqvist *et al.*, *J. Biol. Chem.*, 1993, 268, 20744–20746) contains the model of the ligand with incorrect chirality. We report here the correct model and discuss the relation between this model and the model of the inhibitory complexes between PAP and oxy-anions.

Prostatic acid phosphatase (PAP) is one of the major secretory products of the prostate gland (Ostrowski, 1980). The enzyme is a non-specific phosphomonoesterase hydrolyzing a wide range of alkyl, aryl, and acyl orthophosphate monoesters. Its physiological substrate, however, remains unknown. Like most other non-specific phosphomonoesterases, PAP has the ability to transfer phosphoryl groups to hydroxyl compounds other than water. PAP is an acid phosphatase since it has an optimum pH between 4 and 7. Extensive studies of the catalytic mechanism yield evidence that the enzyme is a histidine phosphatase (Van Etten, 1982; Van Etten *et al.*, 1994; Lindqvist *et al.*, 1994).

Phosphatases are often classified into five groups: (i) alkaline phosphatases, (ii) purple acid phosphatases, (iii) low molecular mass acid phosphatases, (iv) high molecular mass acid phosphatases, and (v) protein phosphatases that are specific for phosphoserine or phosphothreonine residues (Vincent *et al.*, 1992). While there exist a number of excellent inhibitors of phosphatases usually they are not specific and inhibit enzymes from

*Part of this work was supported by the State Committee for Scientific Research (KBN) under grant No. 6P04A 05011.

✉Correspondence should be addressed to: Lukasz Lebioda, Department of Chemistry and Biochemistry, University of South Carolina, Columbia, SC 29208, U.S.A.; fax: 803 777-9521; e-mail: lebioda@psc.psc.sc.edu.

Abbreviation: PAP, prostatic acid phosphatase.

more than one of the groups (Vincent *et al.*, 1992). An exception to this is inhibition by L-(+)-tartrate which is specific for PAP and the homologous proteins like lysosomal acid phosphatase. Initial studies by Abul-Fadl & King (1949) demonstrated that 0.01 M D-tartrate and 0.01 M *meso*-tartrate show no measurable inhibition of PAP whereas 0.01 M L-tartrate and 0.02 M L-tartrate give 94%, and 95% inhibition, respectively. These and subsequent studies demonstrated stereospecificity for L-(+)-tartrate as well as the competitive character of the inhibition.

Kilsheimer & Axelrod (1957) studied inhibition of PAP by using a number of hydroxycarboxylic acids and derivatives of tartaric acid. They concluded that the ability to inhibit is not limited to tartaric acid and is a stereospecific property. The inhibitor must possess a hydroxyl group of the D configuration in the α-position and the β-carbon must be part of a carboxyl group or be attached to a carboxyl or hydroxyl group. L-(+)-Tartrate affinity chromatography is routinely used for PAP purification. The mono-n-propylamide derivative of L-tartaric acid has similar $K_i = 10^{-5}$ as that of L-(+)-tartrate (Van Etten & Saini, 1978).

The specificity of tartrate inhibition was further investigated by Lindqvist *et al.* (1993) who determined the crystal structure of the complex between rat-PAP and L-tartrate at 3.0 Å resolution. Electron density in the shape of an elongated ellipsoid was found in the active site and was attributed to the tartrate ion binding. They modeled the position of the ligand by placing the long axis of the ion along the long axis of the ellipsoid but the density was not good enough to establish the rotational position around the molecular axis. Therefore, they selected an orientation that provided the best hydrogen bonding pattern. The hydrogen bonded contacts of their model are listed in Table 1.

While trying to design better inhibitors of PAP using the tartrate ion as the lead compound we have noticed that the coordinates of the tartrate ion in Lindqvist *et al.* (1993) model, obtained from the Protein Data Bank as entry 1rpa, correspond to D-tartrate rather than the L-tartrate used in the experiment. Therefore, we have replaced the model of the D-tartrate with L-tartrate, placed it in the active site with approximately the same position and optimized the hydrogen bonding pattern. The results of these studies are reported below.

METHODS AND RESULTS

The initial modeling was performed with the program CHAIN (Baylor College of Medicine, 1993). The electron density of L-tartrate ion bound in the active site of rat-PAP is not of sufficient resolution to provide information about its conformation. Therefore, we carried out a search in the Cambridge Structural Data Base (CSD) to explore conformations observed in crystalline state. Also, we created an energy minimized model using the program SYBYL (Tripos, Inc., 1991–1996), which most likely reflects the structure of the ion in the gas phase. Figure 1 shows the superposition of the obtained tartrate structures. The data retrieved from the CSD show that the conformations of the L-tartrate ion are remarkably similar despite different environments. Even the monobenzoyl-L-(+)-tartaric acid, which has a bulky substituent, has similar torsion angles. The different conformation of the energy minimized model is most likely due to the presence of intra-

Table 1. Relevant hydrogen bond contacts

Atoms involved in binding	Distance in the pdb1rpa.ent model of L-tartrate (Å)	Distance in the revised model of L-tartrate (Å)
C1 O11-ARG11 NH1	2.9	2.7
C1 O1-ARG15 NE	2.8	
C1 O1-ARG15 NH2		2.9
C1 O1 HIS12 NE2	2.8	3.0
C2 O2-HIS257 ND1	2.7	2.8
C3 O3-ARG15 NH2	4.0	
C3 O3 ARG15 NE		3.2
C3 O3-ARG79 NH1	2.8	3.1
C4 O5-ARG79 NH1	5.0	3.3

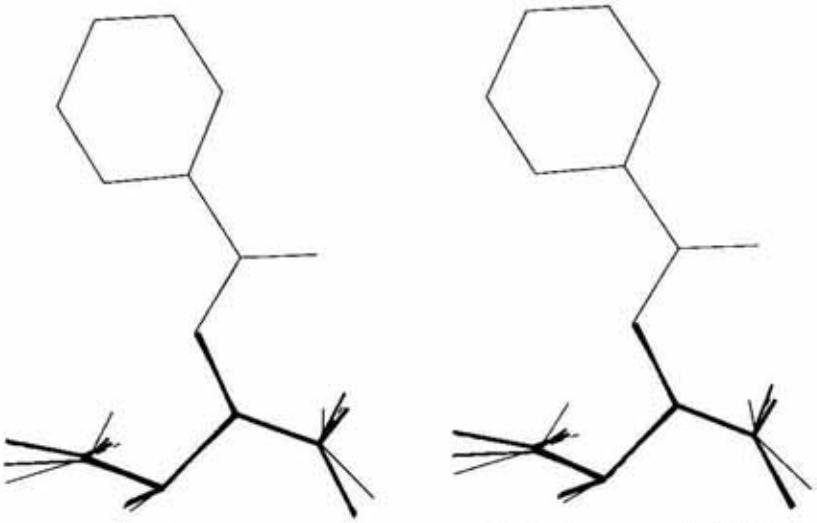

Figure 1. Superposition of 3-(+)-(2*R*,3*R*)-tartaric acid molecules retrieved from Cambridge Structural Data Base (single line, double bold line, and triple bold line) and our revised model of L-(+)-tartrate (dash).

The average torsion angles for these structures are −118 (σ = 12), −174 (σ = 1.0), and −131 (σ = 12).

molecular hydrogen bonding instead of the intermolecular hydrogen bonding and the lack of an environment that would balance the charges of its carboxylates.

The superposition of the active site of PAP with both L-(+) and D-(−)-tartrate ions is shown in Fig. 2. The relevant distances, given in Table 1, show that by using the correct enantiomer we gained two hydrogen bonds. These additional hydrogen bonds provide binding energy which is likely to be responsible for the observed differences in the binding affinities of the L- and D-tartrate ions. Only side chain atoms are involved in tartrate ion binding. Three of them are arginines (residues 11, 15, 79) which are protonated and charged at the pH range in which the enzyme is active. His12, which is the nucleophile in the catalysis, most likely is protected from protonation by the electrostatic field produced by the arginines.

Initially it was proposed that the tartrate ion inhibits PAP because its structure is related to the transition state in which a phosphorus atom is pentacoordinated (Van Etten, 1982). Oxoanions such as vanadate or molybdate are true transition state analogues and bind in the active site covalently through the side chain of His12 (Lindqvist *et al.*, 1994). A superposition of the structure of the complex of PAP-vanadate on the structure of the complex PAP-L-(+)-tartrate is shown in Fig. 3. The positions of the two anions are significantly different. It appears that the tartrate binding is due to the cooperation of two factors. The first is the interaction between the molecular electrostatic potential and the anionic ligand. This factor is not sufficient to induce binding by itself as the other stereomers of tartrate are not effective inhibitors. The other factor is the extensive hydrogen bonding between the L-(+) tartrate ion and the enzyme molecule. These interactions involve a larger part of the active site than binding of the vanadate ion or its analogues and the excellent fit observed appears to be fortuitous. Further analysis of the relation between the substrate and inhibitor has to be deferred until the physiological substrate of PAP is known.

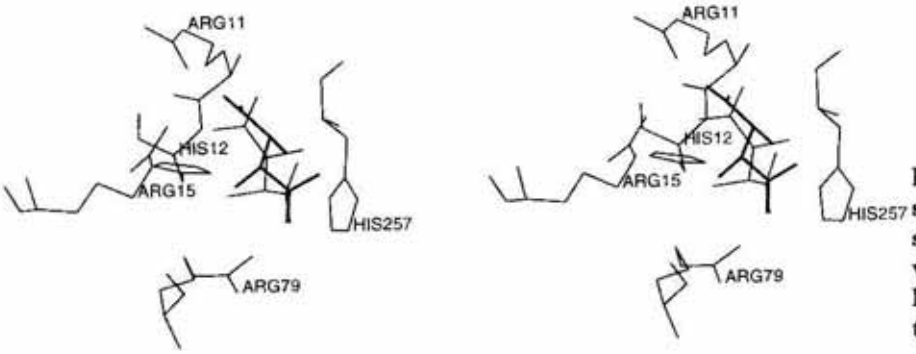

Figure 2. Stereoview of the superposition of the active site of rat PAP (single line) with both L-(+) (double bold line) and D-(-) (single line) tartrate ions.

To estimate significance of electrostatic interactions in inhibitor binding, we calculated

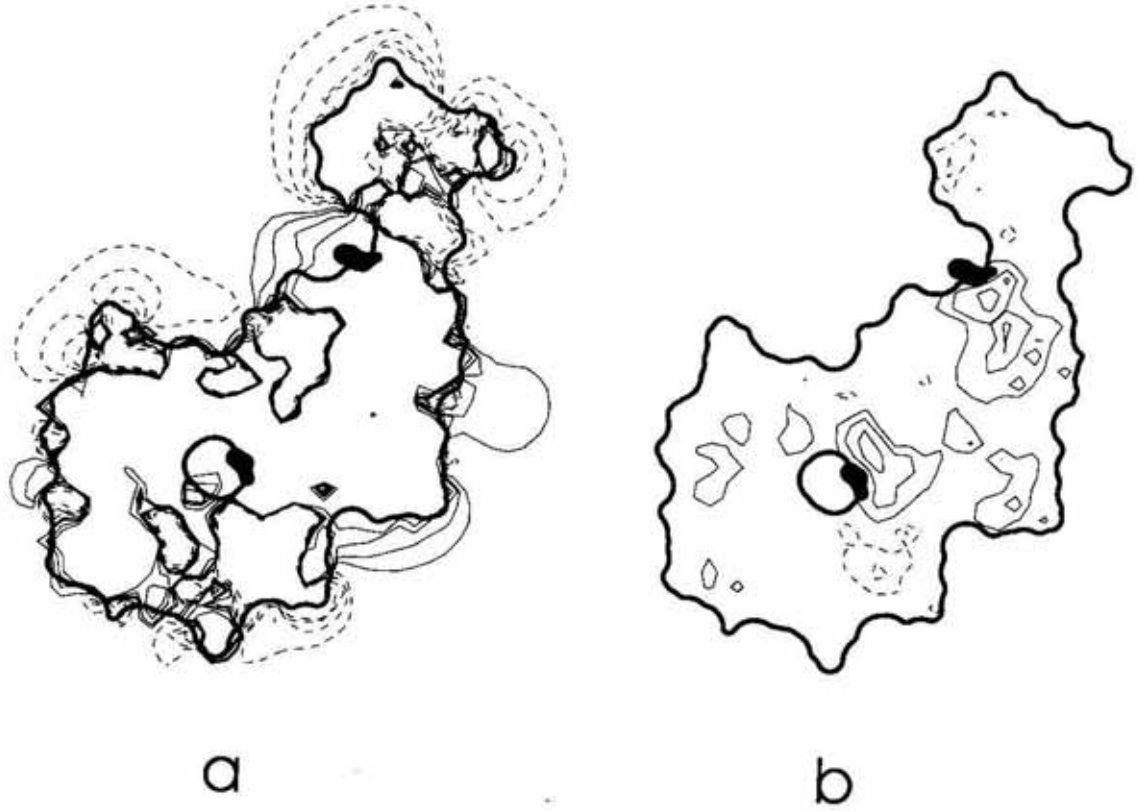

Figure 3. Stereoview of the superposition of rat PAP-vanadate (single line) complex with that of rat PAP-L-(+)-tartrate complex (triple bold line).

electrostatic potentials around the molecule using the DelPhi modul of the INSIGHT II software (Molecular Simulations, San Diego, CA, U.S.A., 1996) to solve the Poisson-Boltzman equation (Gilson *et al.*, 1987; Honig & Nicholls, 1995). Programs from CCP4 package (1994) were used to generate PAP dimer with added hydrogen atoms from coordinates of 1rpa. The atomic partial charges were assigned to all atoms using parameters given by Weiner *et al.* (1986) the dielectric constants inside and outside of the protein surface were set to 2 and 80, respectively, ionic strength was 0.10 M. Figure 4 shows two-dimensional slice through a solvent accessible surface of a dimer. The plane crosses tartrate binding sites in both, perpendicular to each other, protein units. Position of tartare (not used for calculations) is marked as a black object in active site clefts. For clarity, electrostatic potentials on Fig. 4a are contoured at levels 0.5kt, 1kT, 2kt and 4kt while 25kt, 50kt and 75kt on Fig. 4b. Negative potentials is represented by dashed lines and positive by solid lines.

Calculations made for PAP show that the net negative charge on a protein dominates the electrostatic potential around the molecule except in the active site where a cluster of histidines and arginines forms a region of highest positive potential contributing to the binding of anionic ligands. Positive potential

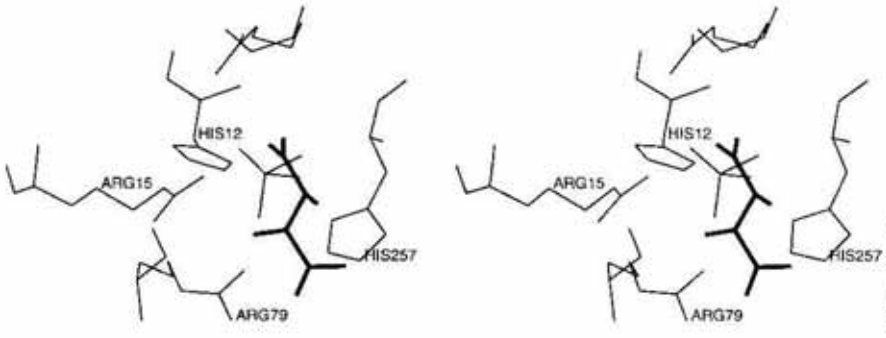

Figure 4. Molecular Electrostatic Potential calculated for the PAP molecule using the DelPhi software.

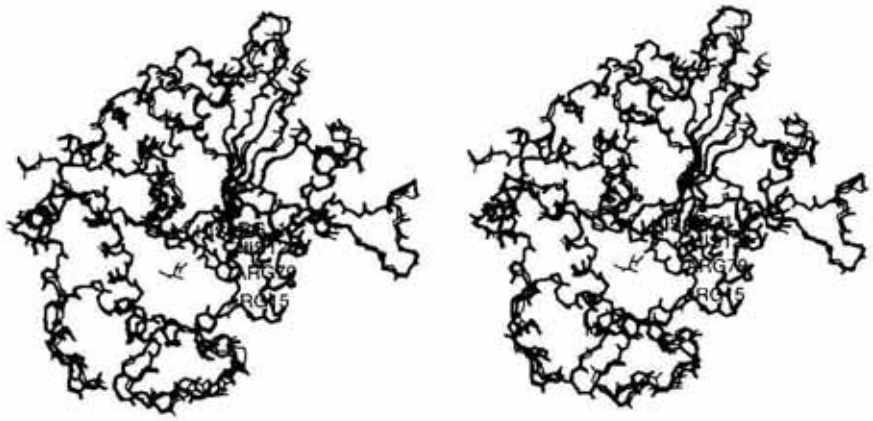

Figure 5. Stereoview of the superposition of the Cα traces of rat PAP (single line) and human PAP (double bold line) with L-(+)-tartrate (single line) in the active site.

is expanding into solvent as a relatively small protrusion surrounded by negative field and attracting anions into active site.

DISCUSSION

Although the structural data used were that for the rat PAP the results are likely to also be valid for the human enzyme. We have recently crystallized human PAP (Kuciel *et al.*, 1992) and determined its structure at 3.1 Å resolution (Jakob *et al.*, 1995). The structure of human PAP shows that the structures of the enzyme from the two sources are very similar as could be expected from the sequence data (75% identity). Figure 5 shows a superposition of the Cα traces of rat and human PAP. The r.m.s. distance between the positions of Cα is 0.62 Å. All residues involved in tartrate binding are highly conserved.

Since the 1950's PAP levels in blood serum have been routinely used to monitor and stage prostate cancer (Gutman & Gutman, 1938). However, recently it has been shown that tests based on prostate-specific antigen (PSA) are superior to PAP in the early detection of prostate cancer (Akino *et al.*, 1995). Although analytical applications of PAP as a routine test to screen for prostate cancer are on the decline, the separation of the phosphatase activity in blood serum into tartrate-inhibitable and tartrate-refractory remains useful. This is especially so as a number of tissues (Drenckhahn *et al.*, 1987) and tumors of non-prostatic origin were found (Bodansky, 1972; Shaw *et al.*, 1981; Sidhu & Sanches, 1993) to express and secrete PAP. The presence of PAP in serum of patients with non-prostatic cancers has not been a factor in the selection of treatment as yet. However, future studies may establish a correlation between effectiveness of particular forms of therapy and the abnormal expression of PAP by cancerous tissues. Thus the design of tartrate related inhibitors of PAP, more potent than the lead compound, remains an attractive and challenging goal.

REFERENCES

Abul-Fadl, A.M. & King, E.J. (1949) Properties of acid phosphatases of erythrocytes and of the human prostate gland. *Biochem. J.* **45**, 51–60.

Akino, H., Tsuka, H., Okada, K., Tsuchiya, Y., Matsubara, M. & Arimura, K. (1995) Value of serum PSA and PAP measurement with newly developed latex turbidimetric immunoassay. *Acta Urologica Japonica* **41**, 439–435.

Bodansky, O. (1972) Acid phosphatase. *Adv. Clin. Chem.* **15**, 143–147.

CHAIN (version 5.4) Manual (1993) Baylor College of Medicine.

COLLABORATIVE COMPUTATIONAL PROJECT, NUMBER 4. (1994) The CCP4 suite: Programs for protein crystallography. *Acta Cryst.* **D50**, 760–763.

Drenckhahn, D., Waheed, A. & Van Etten, R. (1987) Demonstration of prostatic type acid phosphatase in non-lysosomal granules in the crypt epithelium of the human duodenum. *Histochemistry* **88**, 47–52.

Gilson, M.K., Sharp, K.A. & Honig, B.H. (1987) Calculating the elctrostatic potential of molecules in solution: Method and error assessement. *J. Comput. Chem.* **9**, 327–335.

Gutman, E. & Gutman, A.B. (1938) An acid phosphatase occurring in the serum of patients with matastasizing carcinoma of prostate gland. *J. Clin. Invest.* **17**, 473–478.

Honig, B. & Nicholls, A. (1995) A classical electrostatics in biology and chemistry. *Science* **268**, 1144–1149.

Jakob, C.G., Kuciel, R., Lewinski, K., Ostrowski, W. & Lebioda, L. (1995) Crystal structure of human prostatic acid phosphatase at 3.1 Å resolution. *American Cryst. Assoc. Meeting Abstracts*, Montreal, Quebec.

Kilsheimer, G.S. & Axelrod, B. (1957) Inhibition of prostatic acid phosphatase by α-hydroxy carboxylic acids. *J. Biol. Chem.* **227**, 879.

Kuciel, R., Jakob, C.G. & Lebioda, L. (1992) Crystallization of human prostatic acid phosphatase using biphasic systems. *J. Crystal Growth* **122**, 199–203.

Lindqvist, Y., Schneider, G. & Vihko, P. (1993) Three dimensional structure of rat acid phosphatase in complex with L-(+)-tartrate. *J. Biol. Chem.* **268**, 20744–20746.

Lindqvist, Y., Schneider, G. & Vihko, P. (1994) Crystal structures of rat acid phosphatase complexed with the transition-state analogs vanadate and molybdate: Implications for the reaction mechanism. *Eur. J. Biochem.* **221**, 139–142.

Molecular Simulations, INSIGHT II manual (1996) San Diego, U.S.A.

Ostrowski, W. (1980) Human prostatic acid phosphatase: Physicochemical and catalytic properties; in *Male Accessory Glands* (Spring-Mills, E. & Hafez, E.S.F., eds.) pp. 197–213, Elsevier North-Holland Biomedical Press.

Shaw, I.M., Yang, N., Brooks, J.J., Neat, M., Marsh, I. & Seamonds, B. (1981) Immunochemical evaluation of organ specificity of prostatic acid phosphatase. *Clin. Chem.* **27**, 1505–1512.

SYBYL (version 6.3) Manual (1991–1996) Tripos, Inc., St. Louis, U.S.A.

Sindhu, J. & Sanches, R. (1993) Prostatic acid phosphatase in strumal ovary. *Cancer* **72**, 1673–1678.

Van Etten, R.L. (1982) Human prostatic acid phosphatase: A histidine phosphatase. *Ann. N.Y. Acad. Sci.* **390**, 27–51.

Van Etten, R.L. & Saini, M.S. (1978) Selective purification of tartrate-inhibitable acid phosphatase: Rapid and efficient purification (to homogeneity) of human and canine phosphatases. *Clin. Chem.* **24**, 1525–1530.

Van Etten, R.L., Ostanin, K. & Saeed, A. (1994) Heterologous expression of human prostatic acid phosphatase and site-directed mutagenesis of the enzyme active site. *J. Biol. Chem.* **269**, 8971–8978.

Vincent, J.B., Crowder, M.W. & Averill, B.A. (1992) Hydrolysis of phosphate monoesters: A biological problem with multiple solutions. *Trends Biochem. Sci.* **195**, 105–110.

Weiner, S.J., Kolleman, P.A., Nguyen, D.T. & Case, D.A. (1986) An atom force field for simulations of proteins and nucleic acids. *J. Comput. Chem.* **7**, 230–252.